

Infrared physics of the SU(2) Georgi-Glashow crossover transition

Lauri Niemi, Kari Rummukainen, Riikka Seppä and David Weir*

Department of Physics and Helsinki Institute of Physics,

P.O. Box 64, 00014 University of Helsinki, Finland

*E-mail: lauri.b.niemi@helsinki.fi, kari.rummukainen@helsinki.fi,
riikka.seppa@helsinki.fi, david.weir@helsinki.fi*

We perform a lattice study of the phase transition in the SU(2) Georgi-Glashow model in three dimensions, where the gauge symmetry is broken to U(1) by the Higgs mechanism and a photon-like state appears. Due to condensation of monopoles the photon acquires a mass, which depends on the number density of the monopoles. We show that the monopole density can be renormalised on the lattice using gradient flow. Our preliminary results suggest that Polyakov's semiclassical relation between the photon mass and the renormalised monopole density is valid also at the nonperturbative level.

*The 38th International Symposium on Lattice Field Theory, LATTICE2021 26th-30th July, 2021
Zoom/Gather@Massachusetts Institute of Technology*

*Speaker

1. Introduction

Georgi-Glashow gauge theories, where scalar fields transform in the adjoint representation of the gauge group, have a long history of study in particle physics, notably as a grand unified theory when the gauge group is, for example, SU(5) [1]. It also serves as a toy model of nonperturbative physics. In the simple case of a single adjoint scalar and an SU(2) gauge group, the system admits 't Hooft-Polyakov monopole solutions [2, 3] and provides a valuable testing ground for their behaviour. In this simple case, the Higgs mechanism breaks the SU(2) gauge field to a U(1) corresponding to a massless photon. However, monopole condensation gives rise to a small nonzero photon mass [4].

Scalar fields transforming in the adjoint representation of SU(2) are also of interest in theories of physics beyond the Standard Model (BSM). In particular, they allow a more complicated pattern of symmetry breaking phase transitions in the early universe than the minimal Standard Model of the Higgs doublet [5]. Understanding how monopole-like excitations may play a role in BSM phenomenology is crucial, as we go beyond perturbation theory and take the first steps in probing these models with lattice simulations [6].

In this proceedings we explore the phase transition in the SU(2) Georgi-Glashow model in three Euclidean dimensions, which is the high temperature limit of the full (3 + 1)-dimensional theory [7]. This theory also serves as an effective description of hot SU(2) gauge theory in the deconfined phase [8].

Because of monopole condensation, the Higgs regime admits no massless modes and is in fact analytically connected to the confining regime [8, 9]. Semiclassically, the photon mass squared M_γ^2 is expected to be proportional to the monopole gas number density n [4]. We explore this relationship numerically at the nonperturbative level.

While measuring the nonzero photon mass M_γ is relatively straightforward, the monopole number density n is a UV-divergent quantity because of short-lived monopole-antimonopole pairs on the lattice. We show that the monopole number density can be renormalised with the gradient flow [10], so that it has a well-behaved continuum limit. Our results support the hypothesis that the semiclassical relation $M_\gamma^2 \propto n$ is valid for the renormalised n .

1.1 The model in continuum

As outlined above, for our purposes the Georgi-Glashow model consists of SU(2) gauge fields and a Higgs field ϕ in the adjoint representation. By dimensional reduction, its infrared behavior at high temperature is well described by a 3D theory with temperature dependent parameters:

$$S = \int d^3x \left\{ \frac{1}{2} \text{Tr} F_{ij} F_{ij} + \text{Tr} [D_i, \phi]^2 + m_3^2(T) \text{Tr} \phi^2 + \lambda_3(T) (\text{Tr} \phi^2)^2 \right\}. \quad (1)$$

The same 3D action arises as the high-temperature limit of two-color QCD, and of beyond the Standard Model theories involving electroweak triplet scalars. The phase structure depends on two dimensionless ratios,

$$x = \frac{\lambda_3}{g_3^2} \quad \text{and} \quad y = \frac{m_3^2}{g_3^4}, \quad (2)$$

where g_3 is the gauge coupling in 3D.

The monopoles give a mass to the photon-like excitation. Semiclassically [4]

$$M_\gamma^2 \sim \frac{n}{\pi g_3^2}, \quad n \sim \frac{m_W^{7/2}}{g_3} \exp \left[-\frac{4\pi m_W}{g_3^2} f(\lambda_3/g_3^2) \right], \quad (3)$$

where n is a renormalised monopole number density that counts only widely separated monopoles, and $f(z)$ an $\mathcal{O}(1)$ function.

1.2 Lattice formulation

Writing the SU(2) links as U_i , our lattice action reads

$$S = \beta \sum_{x,i < j} \left(1 - \frac{1}{2} \text{Tr} U_{ij}(x) \right) + 2a \sum_{x,i} \left(\text{Tr} \phi(x)^2 - \text{Tr} \phi(x) U_i(x) \phi(x+i) U_i^\dagger(x) \right) + a^3 \sum_x \left(m_L^2 \text{Tr} \phi^2 + \lambda_3 (\text{Tr} \phi^2)^2 \right), \quad (4)$$

where U_{ij} is the plaquette and $\beta = \frac{4}{ag_3^2}$. For small a the mass parameter is related to the continuum one by $m_L^2 = m_3^2 + \delta m^2$, where the counterterm is given in [11]. Letting $\Pi_+ = \frac{1}{2}(\mathbb{1} + \phi/\sqrt{\phi^2})$, a U(1) link variable can be projected out as

$$u_i(x) = \Pi_+(x) U_i(x) \Pi_+(x+\hat{i}). \quad (5)$$

The associated U(1) field-strength tensor is

$$\alpha_{ij}(x) = \frac{2}{g_3 a^{1/2}} \arg \text{Tr} u_i(x) u_j(x+\hat{i}) u_i^\dagger(x+\hat{j}) u_j^\dagger(x). \quad (6)$$

This in turn provides a meaningful definition of the magnetic field B_i on the lattice [12],

$$B_i(x) = \epsilon_{ijk} \alpha_{jk}(x). \quad (7)$$

The magnetic monopole number density is

$$n = \frac{1}{V} \frac{g_3 a^{1/2}}{4\pi} \sum_{x,i} \left| B_i(x+\hat{i}) - B_i(x) \right|. \quad (8)$$

However, it is ultraviolet divergent due to short-lived monopole-antimonopole pairs. We renormalise it with gradient flow of the fields. If we parametrise the links as $U_i(x) = \exp [i\theta_i^c(x)\sigma^c/2]$, the gradient flow for this model in terms of dimensionless flow time τ is

$$\frac{\partial U_i(x)}{\partial \tau} = -ig_3^2 a \frac{\sigma^c}{2} \frac{\partial S}{\partial \theta_i^c(x)} U_i(x) \quad (9)$$

$$\frac{\partial \phi^c(x)}{\partial \tau} = -a^{-1} \frac{\partial S}{\partial \phi^c(x)}. \quad (10)$$

The gradient flow transforms fields towards saddle point configurations of the action, removing ultraviolet fluctuations through smoothing [10]. The smoothing radius ξ in 3D is related to the flow time by $\xi = \sqrt{6\tau}a$.

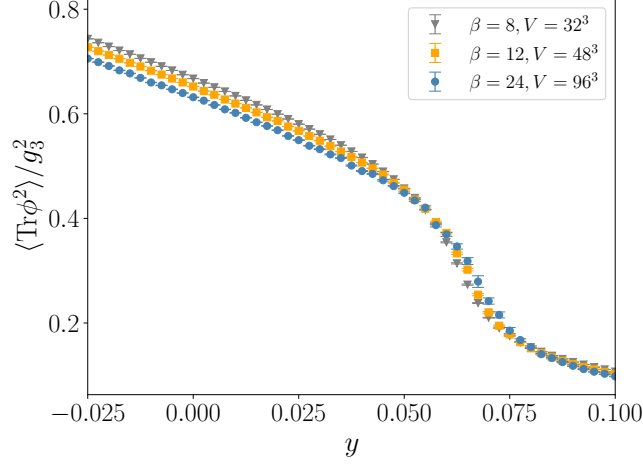


Figure 1: Higgs field expectation value for various lattice spacings, converted to continuum $\overline{\text{MS}}$.

At small a , the Higgs mass parameter m_L^2 requires a large negative counterterm to preserve connection with continuum physics [11]. However, the gradient flow removes UV fluctuations, and effectively reduces the need for the counterterm. Applying the flow to the lattice action (4) with the counterterm included in m_L^2 would drive the Higgs field to larger values as the gradient flow proceeds. To avoid this, we choose the simplest option and explicitly remove the counterterm for the gradient flow and use the continuum mass $m_3^2 = yg_3^4$ instead. This constitutes a choice of the renormalisation scheme, giving us well-behaved results for the monopole number density.

2. Results

We focus on $x = 0.35$, for which the confinement-Higgs transition is of the crossover type in this model [8]. We use the heatbath and over-relaxation algorithms to update the gauge and Higgs fields respectively, and generate field configurations in the canonical ensemble. An additional Metropolis step is added to the Higgs updates for ergodicity.

In Fig. 1, we plot the Higgs field expectation value through the crossover, noting that the renormalised expectation value has a clear continuum limit. The lattice cutoff effects vanish linearly in $1/\beta$ [11]. This allows us to identify the approximate location of the pseudocritical point.

2.1 Renormalised monopole density from gradient flow

As discussed above, we perform gradient flow (see Fig. 2) of the fields on the lattice in order to measure a renormalised monopole number density and remove ultraviolet monopole-antimonopole pairs. In Fig. 3, we show the effect of the gradient flow on the number density of monopoles. We note that the monopoles are screened from each other at long distances, but the lattice needs to be relatively large to capture this effect [9].

The monopoles become heavier as the Higgs condensate grows, and the monopole density drops rapidly. In Fig. 4, we plot both the unrenormalised and renormalised number densities of monopoles for a number of lattice spacings. These results strongly indicate that the renormalised

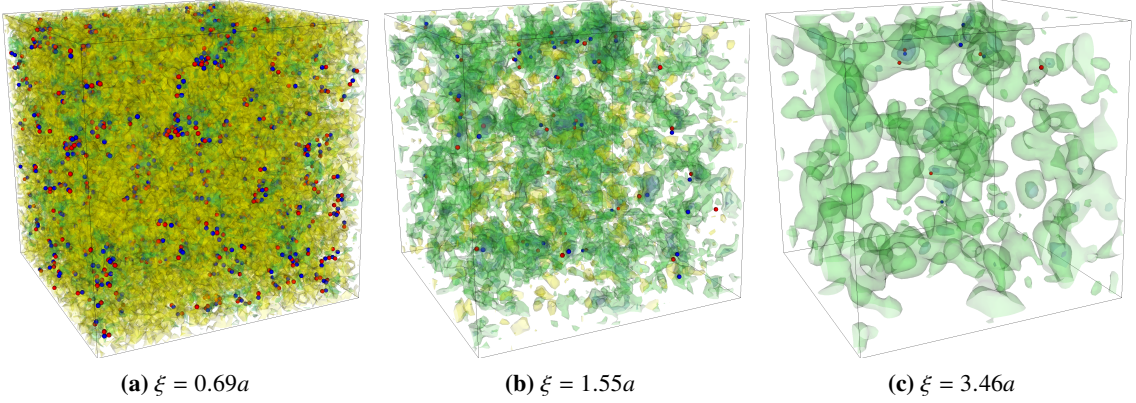


Figure 2: Snapshots of the system at different stages of gradient flow, parameterised by the smoothing radius ξ in terms of the lattice spacing a . Isosurfaces of the Higgs field are shown in shades of green, and (anti)monopoles are shown in red (blue).

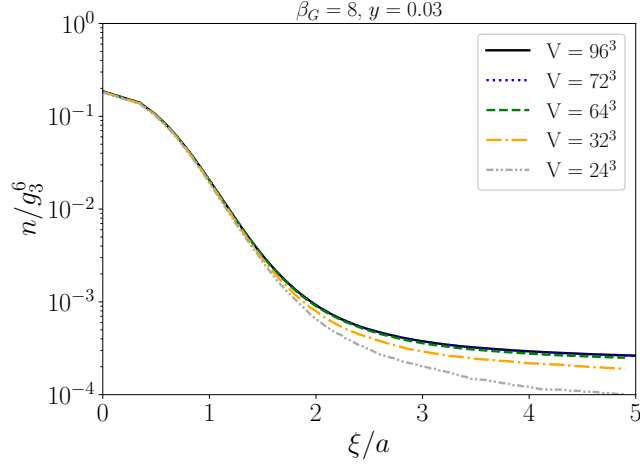


Figure 3: Number density of monopoles n measured as a function of flow time ξ , at fixed β . At small volumes, it seems that all the monopoles annihilate efficiently. As the volume is increased, monopoles experience screening, and one can infer an infinite-volume limit. Note the semilogarithmic scale.

monopole density has a well-defined continuum limit. However, judging from Fig. 3, the lattices used here are likely too small to fully see the screening of monopoles in the infrared. We do not expect this limitation to qualitatively affect the $a \rightarrow 0$ properties of n . A detailed investigation of finite-volume effects will be presented in an upcoming publication.

2.2 Photon mass

We measure the photon mass using blocked correlators at non-vanishing momentum [8]. Within the accuracy of the measurement the photon is massless deep in the Higgs regime, where the monopole gas is dilute. This agrees with the earlier lattice study of [13]. The photon mass squared is approximately proportional to the monopole density, in accordance with semiclassical

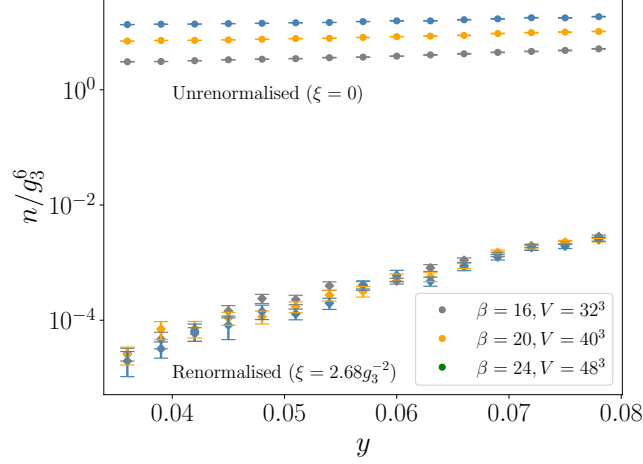


Figure 4: Unrenormalised and renormalised monopole densities at different spacings. The renormalised results, taken at a cooling time of $\xi = 2.68g_3^{-2}$, indicate a well-behaved $a \rightarrow 0$ limit.

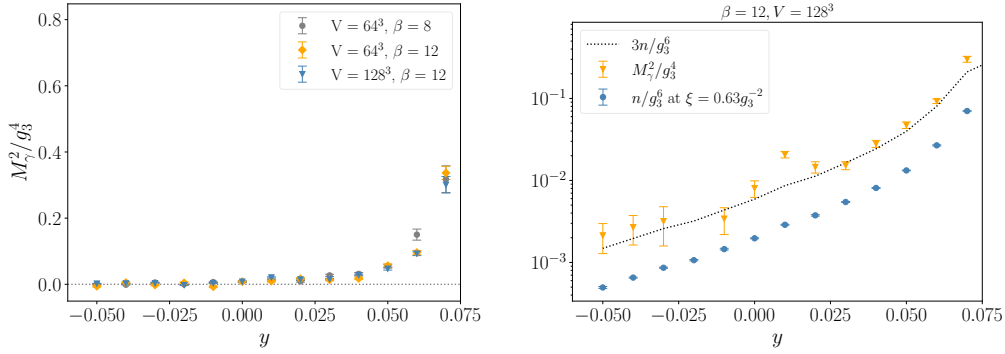


Figure 5: At left, the photon mass squared as a function of y ; the photon becomes almost massless deep in the Higgs phase as expected. At right, the squared photon mass is compared to the renormalised monopole density, for fixed volume and lattice spacing.

expectations. Furthermore, this relationship holds in the crossover region where perturbation theory cannot be relied upon. The proportionality constant depends on how much gradient flow cooling is applied; in other words, it depends on the renormalisation scale.

Our results for the photon mass and its relationship to the monopole number density are shown in Fig. 5.

3. Conclusions

We have measured the monopole number density and photon mass in the SU(2) Georgi-Glashow model. Our results indicate that gradient flow provides a meaningful method of renormalising the monopole number density, giving a result with a well-defined continuum limit.

In addition, we have used blocked correlators to measure the photon mass through the crossover. We have established that the semiclassical proportionality between the monopole number density and the photon mass (3) holds nonperturbatively, and furthermore that it extends to the vicinity of the crossover transition where the semiclassical arguments are not reliable.

For theories beyond the Standard Model which contain adjoint scalar fields, the condensation of monopoles naturally plays a role in crossovers and phase transitions. Our results give qualitative insight into the infrared behaviour of the Higgs regime near the transition point. The presence of monopoles could indeed have consequences for the strength of the transition as previously suggested in Ref. [8]. Due to the nonperturbative nature of processes involving monopoles, caution is warranted when conducting perturbative studies of such models near the transition point, particularly for weak first-order transitions.

References

- [1] H. Georgi and S. L. Glashow, *Phys. Rev. Lett.* **32** (1974), 438-441 doi:10.1103/PhysRevLett.32.438
- [2] G. 't Hooft, *Nucl. Phys. B* **79** (1974), 276-284 doi:10.1016/0550-3213(74)90486-6
- [3] A. M. Polyakov, *JETP Lett.* **20** (1974), 194-195 PRINT-74-1566 (LANDAU-INST).
- [4] A. M. Polyakov, *Nucl. Phys. B* **120** (1977), 429-458 doi:10.1016/0550-3213(77)90086-4
- [5] H. H. Patel and M. J. Ramsey-Musolf, *Phys. Rev. D* **88** (2013), 035013 doi:10.1103/PhysRevD.88.035013 [arXiv:1212.5652 [hep-ph]].
- [6] L. Niemi, M. J. Ramsey-Musolf, T. V. I. Tenkanen and D. J. Weir, *Phys. Rev. Lett.* **126** (2021) no.17, 171802 doi:10.1103/PhysRevLett.126.171802 [arXiv:2005.11332 [hep-ph]].
- [7] T. Appelquist and R. D. Pisarski, *Phys. Rev. D* **23** (1981), 2305 doi:10.1103/PhysRevD.23.2305
- [8] K. Kajantie, M. Laine, K. Rummukainen and M. E. Shaposhnikov, *Nucl. Phys. B* **503** (1997), 357-384 doi:10.1016/S0550-3213(97)00425-2 [arXiv:hep-ph/9704416 [hep-ph]].
- [9] A. C. Davis, A. Hart, T. W. B. Kibble and A. Rajantie, *Phys. Rev. D* **65** (2002), 125008 doi:10.1103/PhysRevD.65.125008 [arXiv:hep-lat/0110154 [hep-lat]].
- [10] M. Lüscher, *JHEP* **08** (2010), 071 [erratum: *JHEP* **03** (2014), 092] doi:10.1007/JHEP08(2010)071 [arXiv:1006.4518 [hep-lat]].
- [11] M. Laine, *Nucl. Phys. B* **451** (1995), 484-504 doi:10.1016/0550-3213(95)00356-W [arXiv:hep-lat/9504001 [hep-lat]].
- [12] A. C. Davis, T. W. B. Kibble, A. Rajantie and H. Shanahan, *JHEP* **11** (2000), 010 doi:10.1088/1126-6708/2000/11/010 [arXiv:hep-lat/0009037 [hep-lat]].
- [13] A. Hart, O. Philipsen, J. D. Stack and M. Teper, *Phys. Lett. B* **396** (1997), 217-224 doi:10.1016/S0370-2693(97)00104-4 [arXiv:hep-lat/9612021 [hep-lat]].